nature neuroscience

Large-scale remapping of visual cortex is absent in adult humans with macular degeneration

Heidi A Baseler[1], André Gouws[1,6], Koen V Haak[2,6], Christopher Racey[1], Michael D Crossland[3,4], Adnan Tufail[3,4], Gary S Rubin[3], Frans W Cornelissen[2] & Antony B Morland[1,5]

The occipital lobe contains retinotopic representations of the visual field. The representation of the central retina in early visual areas (V1–3) is found at the occipital pole. When the central retina is lesioned in both eyes by macular degeneration, this region of visual cortex at the occipital pole is accordingly deprived of input. However, even when such lesions occur in adulthood, some visually driven activity in and around the occipital pole can be observed. It has been suggested that this activity is a result of remapping of this area so that it now responds to inputs from intact, peripheral retina. We evaluated whether or not remapping of visual cortex underlies this activity. Our functional magnetic resonance imaging results provide no evidence of remapping, questioning the contemporary view that early visual areas of the adult human brain have the capacity to reorganize extensively.

The human brain contains maps of the retina on the surface of the occipital lobes[1]. Abnormal visual development can modify these retinotopic maps[2–5]. Under circumstances in which individuals acquire early visual experience in the presence of a lesion to the center of the retina, reorganization of the visual representation occurs[6]. The visual brain in these individuals remaps by allocating a larger than normal area of cortex to intact, peripheral vision. Although brain plasticity is clearly possible when neural changes occur early in life, the adult brain also appears to be capable of plasticity. Experimentally induced retinal lesions in adult animals can lead to a remapping of primary visual cortex to respond to inputs from nearby intact retina[7–13]. We sought to determine whether cortical remapping generalizes to humans who acquire retinal lesions in adulthood.

Several groups have investigated reorganization in human adult cortex when retinal lesions were acquired as a result of disease (macular degeneration). These studies have produced variable results, generating some controversy. One group[14] found no evidence of activity in parts of visual cortex that normally receive input from lesioned retina (the lesion projection zone) in a single, elderly individual. Another study[15], on the other hand, reported widespread activation of the lesion projection zone in two adults with juvenile macular degeneration and suggested that this might reflect a cortical remapping via horizontal connections similar to, but larger than, those found in earlier animal studies. The remapping hypothesis is supported by another functional magnetic resonance imaging (fMRI) study claiming that activation of deprived cortex can be generated by eccentric fixation[16]. Stimulating the occipital cortex of an individual blinded in adulthood by trauma to the optic nerves resulted in abnormal phosphene maps, also suggesting cortical remapping[17]. Despite these reports, the implication that remapping is responsible for the large-scale spread of activation in the lesion projection zone of individuals with retinal lesions acquired in adulthood has been seriously questioned[18–20].

Using methods that explicitly evaluate visual cortical maps, we sought to determine whether humans with lesions acquired in adulthood exhibit reorganization in the form of cortical remapping of visual input over the large-scale seen in individuals with congenital foveal loss of vision[6]. In contrast with prior studies largely restricted to a few individuals with juvenile forms of macular degeneration (JMD), we compared responses in a large number of individuals in two different age groups: those with JMD and those with the more common age-related form (AMD), and their age-matched controls. We found no evidence of large-scale remapping in early visual areas in adults with acquired retinal lesions. Indeed, the area of activity in primary visual cortex measured in these individuals was no different from that predicted on the basis of normal retinotopic maps. Furthermore, the absence of cortical remapping was not dependent on the age at which the individuals acquired retinal lesions in adulthood.

RESULTS

Cortical responses were measured in 16 individuals with macular degeneration (see **Table 1**) and 12 age-matched controls with normal vision using fMRI. Individuals with macular degeneration had bilateral lesions for at least 1 year and had developed a stable preferred retinal locus that allows good fixation performance. We tested two age groups: young (mean age = 30) and elderly (mean age = 76). Participants passively viewed flickering checkerboard stimuli configured in a ring that expanded through increasing eccentricity or a wedge that rotated around a central point. Such stimuli reliably modulate blood oxygenation level–dependent signals and are used to map visual areas in occipital cortex[1,21–24]. Response magnitude was

[1]York Neuroimaging Centre, Department of Psychology, University of York, York, UK. [2]Laboratory for Experimental Ophthalmology and BCN Neuroimaging Centre, University Medical Centre Groningen, University of Groningen, Groningen, The Netherlands. [3]Institute of Ophthalmology, University College London, London, UK. [4]Moorfields Eye Hospital NHS Foundation Trust, London, UK. [5]Hull-York Medical School, York, UK. [6]These authors contributed equally to this work. Correspondence should be addressed to A.B.M. (a.morland@psychology.york.ac.uk).

Received 22 September 2010; accepted 28 February 2011; published online 27 March 2011; doi:10.1038/nn.2793

Table 1 Summary of affected individuals in the study

Diagnosis	Sex	Age (years)	Eye tested	Lesion diameter (°)	Acuity (logMAR)	BCEA (°)
AMD	F	90.9	Right	9	0.92	17.7
AMD	F	83.5	Right	8	0.98	12.43
AMD	F	81.8	Left	7	0.54	17.7
AMD	M	76.3	Left	6	0.36	8.26
AMD	M	80.2	Left	10	1.06	15.16
AMD	F	70.8	Left	4	0.9	12.37
AMD	M	83.8	Left	15	0.86	20.37
AMD	M	80.6	Right	13	0.76	5.33
Stargardt's	M	19.8	Left	5	0.74	11.71
Stargardt's	F	19.7	Left	3	1.02	2.24
Stargardt's	M	49.5	Right	6	0.56	14.47
Stargardt's	F	41.2	Right	10	0.9	1.69
Stargardt's	F	34.7	Right	8	1.08	13.54
Stargardt's	F	39.4	Right	9	0.98	18.11
Stargardt's	F	24.3	Left	3.5	0.66	9.33
Stargardt's	M	35.8	Left	17	1.12	13.26

BCEA, bivariate contour ellipse area (a measure of fixation ability using microperimetry); logMAR, log(minimum angle of resolution).

first evaluated using coherence as an outcome measure, as in previous similar fMRI studies[18,25] (Online Methods).

We made coherence maps for each of the individuals in the two groups, those with macular degeneration (the patient group) and the age-matched controls (the control group). Although control subjects showed substantial visually driven responses throughout visual cortex, both the young and elderly patient groups only displayed substantial responses in the anterior occipital lobe. Strong responses in these individuals are therefore limited to regions of the cortex that normally map peripheral (that is, intact) retina (**Fig. 1**).

Responses in the lesion projection zone were compared quantitatively with those in regions that are normally driven by intact retina using regions of interest (ROIs) defined anatomically to avoid any bias toward activation patterns. In both hemispheres, one region was selected at the occipital pole, normally representing the central visual field, and another region in the fundus of the calcarine sulcus, normally representing more peripheral locations. The BOLD signal plotted as a function of time showed robust modulations in response to stimulus onset at both the occipital pole and calcarine sulcus in controls (**Fig. 1**). Clear differences in the response latency of the signals measured at the occipital pole and calcarine sulcus reflect the normal retinotopic mapping of early visual areas. Fourier analysis was also applied to the average time series (**Fig. 1**). The resultant spectra (and associated z scores) are consistent with the time series, showing robust signals at the stimulation frequency at both cortical locations in the control group, but only at the calcarine sulcus in the patient group.

Group effects

Our data analysis (**Fig. 1**) captured responses in individuals and conformed to the approach used in previous work on a limited number of cases[15,18,26]. Extending our analysis to the group level, we categorized participants according to age and visual status (young and elderly, patient and control). Responses were assessed at three cortical locations: the two mentioned above (calcarine sulcus and occipital pole; **Fig. 1**), and a third control region located further anterior in the brain in non-visual cortex, chosen to serve as a baseline measure.

The results for the elderly group are shown in **Figure 2a**. We performed a two-way analysis of variance (ANOVA) with visual status (patient versus control group) and ROI (calcarine sulcus versus occipital pole versus control region) as main factors. A significant main effect was found for both visual status ($F = 8.62$, $P < 0.01$) and brain region ($F = 24.20$, $P < 10^{-6}$), with a significant interaction ($F = 3.30$, $P < 0.05$). *Post hoc* tests (corrected for multiple comparisons) revealed a significant difference between the patient and control groups at the occipital pole ($P < 0.01$), but none at the calcarine sulcus or at the control region. In the patient group, signals at the occipital pole were not significantly different from the baseline measure at the control region ($P > 0.05$), but were significantly different from signals from the intact retina at the calcarine sulcus ($P < 0.001$). Patient group responses at the calcarine sulcus were robust and well above baseline ($P < 0.001$). In the control group, signals at the occipital pole and calcarine sulcus were not significantly different from one another ($P > 0.05$), but both differed significantly from the baseline response (calcarine sulcus versus control region, $P < 0.001$; occipital pole versus control region, $P < 0.05$).

Previous work that revealed activity in the lesion projection zone primarily tested individuals who acquired lesions earlier in adulthood than the individuals with AMD that we examined. Comparing the young patient group with the young control group, however, yielded the same results as in the elderly patient group (**Fig. 2b**), with significant main effects of visual status ($F = 52.32$, $P < 10^{-7}$) and ROI ($F = 95.72$, $P < 10^{-15}$) and a significant interaction between them ($F = 18.36$, $P < 10^{-5}$). *Post hoc* tests (corrected) also revealed the same pattern of results as in the elderly groups, but with all differences achieving significance at $P < 0.001$. Large-scale remapping appears to be absent independent of the age in adulthood at which the retinal lesions are acquired.

To test the reproducibility of our results, we acquired additional data on a separate day in most participants ($n = 20/28$) and found

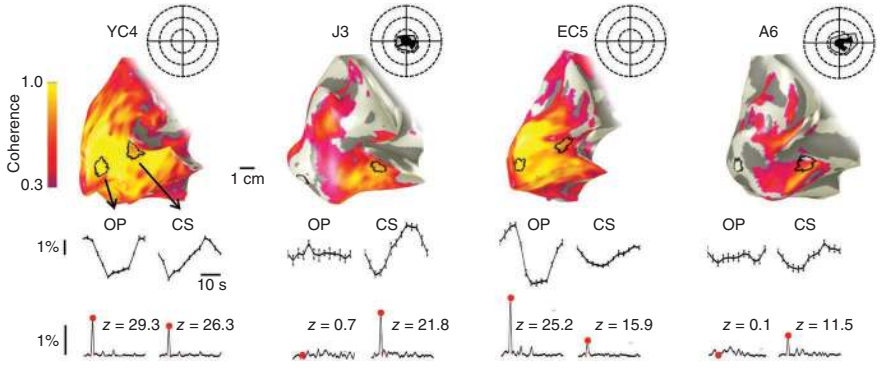

Figure 1 Cortical responses to visual stimulation. BOLD responses for four individuals (from left to right): a young control subject (YC4, age 30), a young patient (J3, age 49), an elderly control subject (EC5, age 66) and an elderly patient (A6, age 70). Visual field results from microperimetry for each subject are inset to the right of each brain image and indicate absolute (black) and partial (gray) scotoma. Dotted concentric circles represent 5, 10 and 15 deg eccentricity. BOLD response coherence is encoded in color and superimposed on smoothed, left occipital lobes. Single cycle time series averages are shown for the two occipital ROIs representing central (occipital pole, OP) and more peripheral retina (calcarine sulcus, CS). Fast Fourier transforms were performed on each full time series and amplitude spectra are also shown for each ROI; stimulus frequency (seven cycles per scan) is indicated by the red dot. z scores indicate the number of s.d. the FFT amplitude at the stimulus frequency differs from the distribution of all of the other frequency amplitudes.

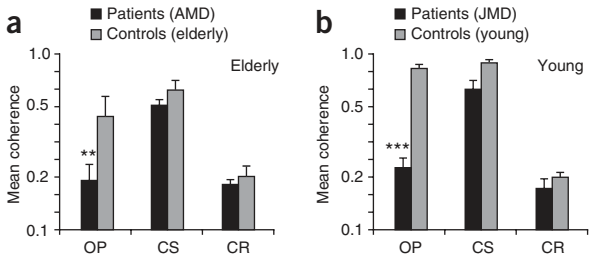

Figure 2 Mean coherences for each ROI, averaged across individuals for each group. CR, control region in nonvisual cortex. Error bars indicate standard error. $***P < 0.001$, $**P < 0.01$. (**a**) Elderly patients (AMD) versus elderly controls. (**b**) Young patients (JMD) versus young controls.

that the data conformed to the same pattern. Repeated-measures ANOVA revealed no main effect of session in all groups ($P > 0.05$). Combining data across sessions, we also tested explicitly for statistical differences associated with age across groups. A three-way ANOVA was performed on the elderly and young groups, with ROI, visual status and age as factors. As in the individual age groups, significant main effects of visual status ($F = 23.40$, $P < 10^{-5}$) and ROI ($F = 60.00$, $P < 10^{-15}$) were found, as well as a significant interaction between them ($F = 7.18$, $P < 0.01$). There was also a main effect of age ($F = 8.82$, $P < 0.01$), a feature that we have noted previously[27]. However, there were no significant interactions between age and visual status ($F = 2.09$, $P = 0.15$) or age and ROI ($F = 2.31$, $P = 0.11$). Thus, although age affects the overall magnitude of fMRI responses, it does so similarly in both the patient and control groups and does not alter the pattern of differences found between them.

Simulating retinal lesions in controls

Using a control region in a nonvisual brain area as a baseline measure comes with the danger that small, but genuine, occipital signals may escape detection, for example, if signal-to-noise ratios vary across the brain[28] or if the control region is in fact responsive to visual stimuli. To improve the specificity of our measurements, we compared signals in the same region of visual cortex (the occipital pole) in control subjects in the presence or absence of visual stimulation. We scanned 12 new control subjects (mean age = 27) while they passively viewed the expanding ring checkerboard stimulus either in full or with a central mask (gray disk radius = 7.5 degrees) simulating a macular lesion (**Fig. 3**). The presence of the central mask in the stimulus largely removes significant responses from the occipital pole.

Using the new baseline measure, we compared responses from the young control group with those from the young patient group and the control group from the first experiment, averaged across sessions (**Fig. 4**). A two-way ANOVA revealed main effects of group (patient versus control versus new control groups, $F = 38.57$, $P < 10^{-9}$) and ROI (occipital pole versus calcarine sulcus, $F = 56.08$, $P < 10^{-8}$), as well as a significant interaction between them ($F = 8.50$, $P < 0.001$). *Post hoc* tests (corrected) showed that these effects were carried by important features at the occipital pole and calcarine sulcus. First, responses at the occipital pole did not differ significantly between the patient group and the new control group shown the simulated scotoma ($P > 0.05$), but both were significantly below those of the original control group shown the full stimulus ($P < 10^{-5}$ for both comparisons). Second, responses at the calcarine sulcus in all three groups were significantly above baseline, as expected ($P < 0.001$). The patient group responses at the calcarine sulcus fell significantly below those of the original age-matched controls ($P < 0.05$). In summary, our results using an improved baseline measure again support the absence of large-scale remapping in individuals with macular degeneration.

Partial volume effects

Even though stimulation of peripheral retina is expected to produce fMRI responses of equal magnitude in both patient and control groups, we noted that signals at the calcarine sulcus were relatively reduced in both the elderly and young patient groups (calcarine sulcus; **Fig. 2**) and significantly so when data were combined across sessions ($P < 0.05$; **Fig. 4**). Because lesion size was variable across the patient group, the anatomically defined ROI at the calcarine sulcus could include tissue in the lesion projection zone, effectively reducing the signal there. Such 'partial volume' effects are therefore predicted to be more likely when retinal lesions are large.

A multiple regression was performed with lesion size (mean lesion diameter; **Table 1**) and age as regressors, as age was shown previously to have a negative effect on fMRI responses (see above). The analysis revealed an overall significant relationship between lesion size, age and response (coherence) at the calcarine sulcus ($R^2 = 0.308$, $P < 0.05$). Consistent with the partial volume prediction, the effect was carried entirely by lesion size (t(one-tailed) = −1.95, $P = 0.036$) rather than age (t(one-tailed) = −0.74, $P = 0.238$). In contrast, no such

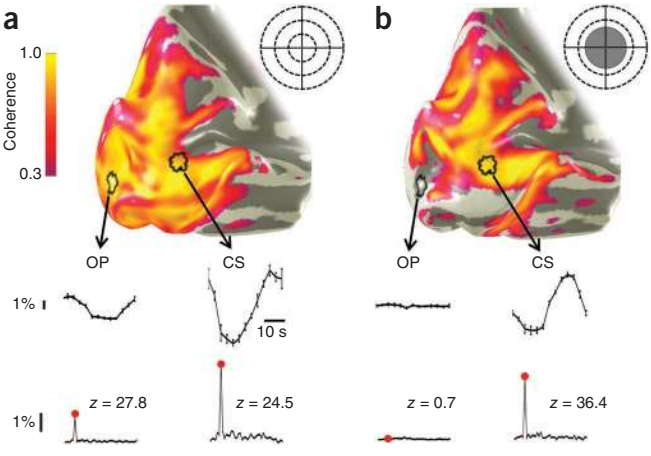

Figure 3 Simulating retinal lesions in a control subject. In both panels, the left occipital lobe of a control subject is shown with BOLD signal coherence superimposed on the surface. Below each panel time series (averaged to a single stimulus cycle) and amplitude spectra of the time series are given for circular regions of cortex at the occipital pole and calcarine sulcus. (**a**) Response to expanding checkerboard ring stimulus spanning full field. (**b**) Response to same stimulus as in **a**, but with central ±7.5 deg masked with a uniform, mean luminance gray disc. Data are presented as in **Figure 1**.

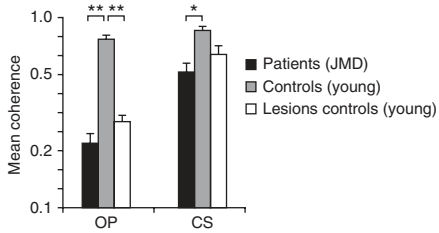

Figure 4 Occipital lobe responses compared across groups and ROIs. Mean coherences averaged across sessions and across individuals from three groups: young patient data from experiment 1, young control data from experiment 1 and lesion control group data from experiment 2 using new baseline measure at the occipital pole in response to stimulus with central ±7.5 deg masked with uniform gray. $**P < 0.01$, $*P < 0.05$. Error bars indicate s.e.m.

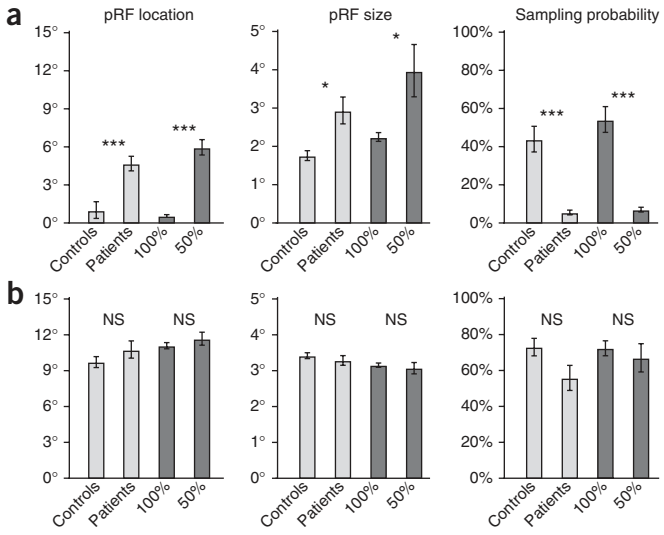

Figure 5 Receptive field characteristics. (**a**,**b**) Population receptive field (pRF) characteristics in the lesion projection zone (**a**) and the calcarine sulcus (**b**). Mean pRF locations and sizes and the sampling probability (percent voxels exceeding 15% variance explained) are shown. Light gray bars show data for individuals with macular degeneration and age-matched controls. Data are given for combined age groups, as none of the outcome measures showed group contrasts (patient group versus control group) that were specific to age (location, $F = 0.27$, $P = 0.603$; size, $F = 3.36$, $P = 0.074$; sampling probability, $F = 0.27$, $P = 0.603$). In two patients, we were unable to derive population receptive field estimates in the lesion projection zone. Dark gray bars show data for controls that were presented the unmasked (100%) stimulus or the stimulus simulating a central scotoma (50% masked). $*P < 0.05$, $***P < 0.001$. Error bars refer to s.e.m.

relationship was found in regions where no response was predicted and partial volume effects were less likely, either well inside the lesion projection zone at the occipital pole ($R^2 = 0.059$, $P = 0.336$) or at the control region in nonvisual cortex ($R^2 = 0.055$, $P = 0.346$).

Receptive field characteristics

Although there were no significant group differences in occipital pole signals between the patient group and the control group with simulated retinal lesions, there was a hint that occipital pole signals in both groups may exceed those found in the control region (**Fig. 2**). It is possible that these signals are visually driven by a small proportion of neurons with large and/or eccentric receptive fields[19,29] that extend into areas of stimulated retina.

To investigate the properties of potential visually driven signals, we modeled population receptive fields[30] of responses in an enlarged region centered on the occipital pole region described above (Online Methods; **Supplementary Results** and **Supplementary Fig. 1**). The mean population receptive field location and size around the occipital pole were abnormally large in both the patient group (location, $t = 3.81$, $P < 0.001$; size, $t = 2.90$, $P = 0.01$) and the control group when central retinal lesions are simulated (location, $t = 7.90$, $P < 0.001$; size, $t = 2.44$, $P = 0.032$) (**Fig. 5**). The significant shift in population receptive field location (**Fig. 5a**) implies an apparent shift in the representation of these voxels, that is, rendering them 'ectopic'. In contrast, population receptive fields in the calcarine sulcus region (**Fig. 5**) did not differ significantly either between the patient and control groups (location, $t = 1.09$, $P = 0.285$; size, $t = 0.72$, $P = 0.481$) or between masked and unmasked conditions for the controls (location, $t = 0.84$, $P = 0.414$; size, $t = 0.44$, $P = 0.669$). Fixation instability in the patient group cannot account for the effects observed, as the patient and control groups with simulated lesions showed similar results and both the occipital pole and calcarine sulcus regions would be affected[5], which they clearly were not.

Cortical representation

Using phase encoded stimuli also allows the cortical mapping of retinal coordinates to be assessed at an individual level. **Figure 6** shows fMRI response maps in the occipital lobes of several individuals in the elderly and young groups. Although subjects with normal vision showed complete retinal representations throughout the occipital lobes (**Fig. 6a**), individuals with macular degeneration showed response maps that were consistent with the projection from intact parts of retina only (**Fig. 6b**).

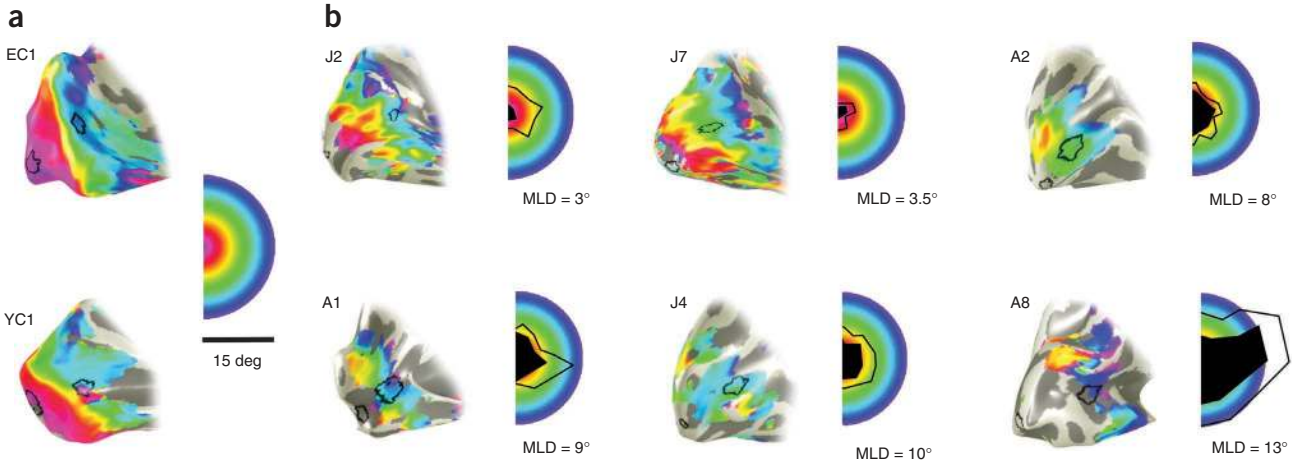

Figure 6 Individual eccentricity maps. (**a**,**b**) FMRI response maps of visual eccentricity superimposed on individual left, partially inflated, occipital lobes for control subjects (**a**) and six affected individuals (**b**). False color is used to indicate the position on the retina (see semi-circular key) to which the cortex is responsive. In **b**, filled black regions of the semicircular key indicate the absolute retinal lesion (scotoma), whereas outlined region exhibits significant, but not absolute, loss of vision. Patient group cortical maps are presented in ascending order (from left to right starting on the top row) of mean lesion diameter (MLD). The cortical representations closely corresponded to the spared retina. Indeed, even retinal locations with reduced sensitivity elicited activity. In all cases, however, the cortical activity did not spread to encompass the occipital pole. Note that this is a different subset of participants than those shown in **Figure 1**.

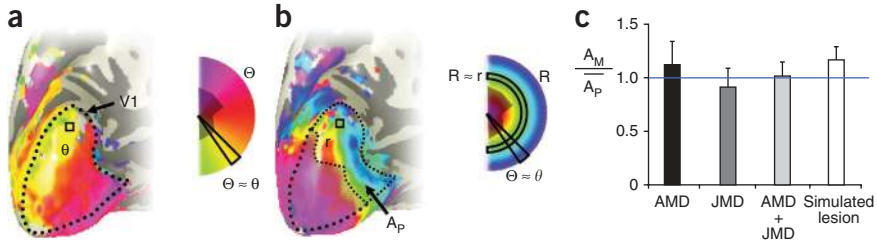

Figure 7 The cortical area representing intact visual field. (**a**,**b**) Schematic of the method by which the area of primary visual cortex representing a subject's intact visual field (measured by microperimetry) is predicted on the basis of normal retinotopic mapping. First, the primary visual cortex boundary was determined in each control participant by identifying the representations of the upper (purple) and lower (green) vertical meridians in calcarine cortex, as indicated by the dotted line on the surface reconstruction of the occipital lobe for one control participant (**a**). Second, we determined whether a voxel (as indicated by the small square in **a** and **b**) has a polar angle phase, θ, that is among the values of polar angle in the intact visual field, Θ (see inset false color map showing the location of the scotoma (shaded) and intact (unshaded) regions). If this is the case, as it is in the illustrated example, we then determined whether the eccentricity represented by the voxel, r, is among the eccentricities in the intact field, R, at the polar angle θ. If the voxel's polar coordinate (r,θ) is among the set of coordinates (R,Θ) of intact visual field locations, the voxel is retained. The predicted cortical area representing the patient's intact visual field, A_P, is then computed from all the retained voxels. For each patient, multiple values of A_P (one for each of the age-matched control retinotopic maps) were obtained and then averaged to compute the mean predicted area of activated V1, $\bar{A}_P$. In each patient, the area of active primary visual cortex, A_M, was also measured. (**c**) The ratio of A_M to $\bar{A}_P$ for the participant groups. No significant differences between groups or between group values and unity were found ($P > 0.05$). Nonsignificant differences from unity present in the AMD and simulated lesion groups are likely the results of the minority of ectopically responding voxels found in **Figure 5**, which could not be predicted from normal retinotopic maps. Error bars indicate s.e.m.

Furthermore, the extent of activation and its phase reflect the size of the spared retina. A large retinal lesion results in a smaller activation area on the brain (for example, A8) and vice versa (for example, J2).

To compare cortical maps quantitatively, we measured the area of activity in the primary visual cortex, A_M, for each patient and control participant with simulated lesions and compared it with a mean predicted area, $\bar{A}_P$, which was determined from the individual's scotoma and normal mappings of age-matched controls (Online Methods and **Fig. 7**). The ratio $A_M/\bar{A}_P$ was compared across participant groups and we found no significant effect of group ($F = 0.81$, $P = 0.46$; **Fig. 7**). Moreover, all groups exhibited ratios that were no different from unity (AMD, $t = 0.59$, $P = 0.57$; JMD, $t = -0.55$, $P = 0.60$; controls, $t = 1.93$, $P = 0.08$), an indication that the area of primary visual cortex activated in all participant groups can be predicted on the basis of normal retinotopic maps. Because each ratio was computed with age-matched control data, patient groups were combined to increase statistical power, but we still found no significant difference between the patient and control groups ($t = -0.81$, $P = 0.41$) or difference from unity in the ratio ($t = 0.14$, $P = 0.89$). Given the variance for patient and control groups in our ratio measure, a significant (at $P < 0.05$) difference in the ratio (of 0.23) would occur if the mean increase in cortical area compared with controls exceeded 160 mm^2 in each hemisphere. This is relatively small compared with the total area of primary visual cortex (~2,500 mm^2, see ref. 31). Our analysis provides strong, quantitative evidence that the extent of early visual cortical activity in the patient and control groups can be predicted on the basis of normal retinotopic maps.

DISCUSSION

Seminal work on early visual deprivation in animals has shown that visual cortex can develop to devote more of its territory to intact visual input at the expense of its representation of impoverished input[32–35]. Such reallocation of cortical processing has also been demonstrated when early visual areas remap following congenital retinal lesions in human[6]. In adulthood, the cortex is less plastic, but even so, remapping of the visual cortical representation has been inferred on the basis of ectopic receptive fields in the lesion projection zone in animal models[7–13]. This effect is, however, rather modest and has been called into question recently[19]. Even so, recent studies of human adults[15,26] suggest a large-scale extension of remapping of the type reported in animal models. We aimed to test explicitly whether or not visual cortical mapping changes following retinal lesions in adult humans. Our results indicate that it does not in three different ways.

First, we found that at the occipital pole, a cortical location that we are certain lies in the lesion projection zone, the signals observed in the patient group are no different than those found in the control group in whom we simulated a central scotoma. The spatially specific ROI analysis has been used extensively previously[15,26] and has been shown to be highly sensitive to remapping[6]. Our result runs contrary to the view that the occipital pole in V1 takes on a new mapping to respond strongly to peripheral stimuli in a way that differs from normal. Previous work in this area has been limited to small numbers of affected individuals and control participants[15,26]. Moreover, previous work has used task-stimulus combinations[15,26] that produced widespread signals in the lesion projection zone in affected individuals, but less in controls, most likely as a result of feedback from extrastriate cortex rather than remapping[18].

Second, our results indicate that throughout the lesion projection zone there are voxels with 'ectopic' receptive fields, but they are equally common and represent the same regions of visual field in both the patient and control group. This finding speaks more generally to the way in which ectopic receptive fields should be interpreted. Frequently, the existence of ectopic receptive fields has been taken as evidence for remapping[7–13]. That ectopic characteristics can be recorded from normally sighted controls challenges this notion, particularly in the context of fMRI research[15,26]. Furthermore, we found that voxels with ectopic receptive fields were not restricted to the fringe of the lesion projection zone, where most electrophysiological measurements have been taken[7–13]. We propose, as have others[19,30], that each cortical location (voxel) contains many neurons, the responses of which can be influenced by stimuli at a range of locations, but that the overall population response is heavily weighted to a modal location. If stimuli are presented only to locations that are a considerable distance from this modal location, the responses of the voxel will be weak, but could be driven by neurons with receptive fields that are large, displaced or large and displaced (see **Supplementary Fig. 1**). We found that only 5–7% of voxels in the lesion projection zone could be classified as responsive, meaning that such signals could escape detection with conventional analyses that average signals over the whole ROI. Notably, the probability of detecting a voxel with ectopic receptive fields is similar to the probability of detecting a neuron with ectopic receptive fields[13]. The ectopic signals in the lesion projection zone may originate from

various sources, including feedback[36–38] and lateral connections[39,40]. Task-specific feedback could elicit more activity in the lesion projections zone in the patient group than in the control group because of the absence of feedforward signals in the patient group[18]. Nevertheless, our results indicate that there is no need to invoke remapping as an explanation of responses in V1 of individuals with macular degeneration.

Third, our study performed for the first time, to the best of our knowledge, a quantitative assessment of the area of cortex driven by intact retina in individuals with retinal disease. The limited size of the patient and control groups coupled with the well-known large variance in visual cortical area across participants[31,41] has prevented such an analysis in previous studies. Our results indicate that the representation of the visual field in V1 in affected individuals can be predicted accurately on the basis of normal retinotopic mapping and that no significant remapping or reorganization was evident. The measures that we derived are sensitive to relatively small changes in cortical maps (<6.5% of V1). This allows us to conclude that there is no remapping of visual cortex over the scale seen in those with congenital central retinal lesions[6]. If neural responses change over time in a very small strip of cortex on the edge of the lesion projection zone, as some have proposed for animal models[7–13], this could escape detection with our analysis. However, we are principally concerned with a large-scale extension of this type of remapping, which we conclude does not exist in humans with central retinal lesions acquired in adulthood.

Consistent with our results, some previous studies on individuals have also found no evidence of remapping of primary visual cortex following retinal damage. A study using cytochrome oxidase to measure activity in an individual with macular degeneration and in macaque models of visual deafferentation found no long-term changes in primary visual cortical organization[42]. Using fMRI and retinotopic mapping methods similar to our own, no activation was found in the lesion projection zone in another individual with macular degeneration[14]. It has been proposed that this negative finding could be a result of the spared foveal vision that this individual exhibited[26]. With this in mind, we only included individuals with central lesions without foveal sparing. A combined fMRI and multiunit neurophysiological study in a carefully controlled animal model (homonymous retinal, but not macular, lesions induced in adult macaques) also showed no long-term changes that would indicate remapping of visual cortex[25]. A recent report of a case series of four individuals with age-related macular degeneration and four with the juvenile form also indicates limited reorganization, but explicit mapping experiments to assess group differences in cortical mapping quantitatively were not undertaken[43]. Having assessed retinotopic maps quantitatively in 16 affected individuals, we are confident that the absence of cortical remapping following retinal lesions in adulthood is a general finding.

The stability of visual organization that we observed may prove to be beneficial. Many of the most promising treatments aimed at restoring vision at the retinal level, such as anti-angiogenic injections, retinal prosthetics and stem-cell therapy, rely on the assumption that cortical circuitry remains largely unchanged. That we can detect no functional abnormality in the visual cortex of affected individuals is reassuring. However, the long-term removal of the principal input to visual cortex can give rise to a reduction in cortical volume[44]. It therefore remains to be seen if neurons in the lesion projection zone can process input normally once it is restored.

METHODS

Methods and any associated references are available in the online version of the paper at http://www.nature.com/natureneuroscience/.

Note: Supplementary information is available on the Nature Neuroscience website.

ACKNOWLEDGMENTS

We would like to thank all of our participants. We thank Edward Silson for constructive discussion of the manuscript. We are also grateful to the Medical Research Council for funding this study (G0401339). K.V.H. and F.W.C. were supported by a grant from Stichting Nederlands Oogheelkundig Onderzoek and by European Union grants #043157 (Syntex) and #043261 (Percept). A.T., G.S.R. and M.D.C. also received financial support from the Department of Health through an award made by the National Institute for Health Research to Moorfields Eye Hospital National Health Service (NHS) Foundation Trust and University College London Institute of Ophthalmology for a Specialist Biomedical Research Centre for Ophthalmology. The views expressed in this publication are those of the authors and not necessarily those of the NHS, the National Institute for Health Research, the Department of Health or the EU commission.

AUTHOR CONTRIBUTIONS

H.A.B. and A.G. acquired and analyzed the neuroimaging data and prepared the manuscript. K.V.H. designed and implemented an analysis to determine the population receptive field characteristics and prepared the manuscript. C.R. acquired neuroimaging data. M.D.C. recruited patients, acquired and analyzed clinical data. A.T. recruited and assessed patients. G.S.R. jointly designed the study, recruited patients and acquired and analyzed clinical data. F.W.C. designed an analysis to determine the population receptive field characteristics and prepared the manuscript. A.B.M. jointly designed the study, acquired and analyzed the neuroimaging data and prepared the manuscript. All authors contributed to drafts of the manuscript.

COMPETING FINANCIAL INTERESTS

The authors declare no competing financial interests.

Published online at http://www.nature.com/natureneuroscience/.
Reprints and permissions information is available online at http://npg.nature.com/reprintsandpermissions/.

1. Wandell, B.A., Dumoulin, S.O. & Brewer, A.A. Visual field maps in human cortex. *Neuron* **56**, 366–383 (2007).
2. Morland, A.B., Baseler, H.A., Hoffmann, M.B., Sharpe, L.T. & Wandell, B.A. Abnormal retinotopic representations in human visual cortex revealed by fMRI. *Acta Psychol. (Amst.)* **107**, 229–247 (2001).
3. Hoffmann, M.B., Tolhurst, D.J., Moore, A.T. & Morland, A.B. Organization of the visual cortex in human albinism. *J. Neurosci.* **23**, 8921–8930 (2003).
4. Muckli, L., Naumer, M.J. & Singer, W. Bilateral visual field maps in a patient with only one hemisphere. *Proc. Natl. Acad. Sci. USA* **106**, 13034–13039 (2009).
5. Levin, N., Dumoulin, S.O., Winawer, J., Dougherty, R.F. & Wandell, B.A. Cortical maps and white matter tracts following long period of visual deprivation and retinal image restoration. *Neuron* **65**, 21–31 (2010).
6. Baseler, H.A. *et al.* Reorganization of human cortical maps caused by inherited photoreceptor abnormalities. *Nat. Neurosci.* **5**, 364–370 (2002).
7. Kaas, J.H. *et al.* Reorganization of retinotopic cortical maps in adult mammals after lesions of the retina. *Science* **248**, 229–231 (1990).
8. Heinen, S.J. & Skavenski, A.A. Recovery of visual responses in foveal V1 neurons following bilateral foveal lesions in adult monkey. *Exp. Brain Res.* **83**, 670–674 (1991).
9. Chino, Y.M., Kaas, J.H., Smith, E.L. III, Langston, A.L. & Cheng, H. Rapid reorganization of cortical maps in adult cats following restricted deafferentation in retina. *Vision Res.* **32**, 789–796 (1992).
10. Gilbert, C.D. & Wiesel, T.N. Receptive field dynamics in adult primary visual cortex. *Nature* **356**, 150–152 (1992).
11. Darian-Smith, C. & Gilbert, C.D. Topographic reorganization in the striate cortex of the adult cat and monkey is cortically mediated. *J. Neurosci.* **15**, 1631–1647 (1995).
12. Kaas, J.H. Sensory loss and cortical reorganization in mature primates. *Prog. Brain Res.* **138**, 167–176 (2002).
13. Giannikopoulos, D.V. & Eysel, U.T. Dynamics and specificity of cortical map reorganization after retinal lesions. *Proc. Natl. Acad. Sci. USA* **103**, 10805–10810 (2006).
14. Sunness, J.S., Liu, T. & Yantis, S. Retinotopic mapping of the visual cortex using functional magnetic resonance imaging in a patient with central scotomas from atrophic macular degeneration. *Ophthalmology* **111**, 1595–1598 (2004).
15. Baker, C.I., Peli, E., Knouf, N. & Kanwisher, N.G. Reorganization of visual processing in macular degeneration. *J. Neurosci.* **25**, 614–618 (2005).
16. Schumacher, E.H. *et al.* Reorganization of visual processing is related to eccentric viewing in patients with macular degeneration. *Restor. Neurol. Neurosci.* **26**, 391–402 (2008).
17. Cowey, A. & Walsh, V. Magnetically induced phosphenes in sighted, blind and blindsighted observers. *Neuroreport* **11**, 3269–3273 (2000).

18. Masuda, Y., Dumoulin, S.O., Nakadomari, S. & Wandell, B.A. V1 projection zone signals in human macular degeneration depend on task, not stimulus. *Cereb. Cortex* **18**, 2483–2493 (2008).
19. Wandell, B.A. & Smirnakis, S.M. Plasticity and stability of visual field maps in adult primary visual cortex. *Nat. Rev. Neurosci.* **10**, 873–884 (2009).
20. Masuda, Y. *et al.* Task-dependent V1 responses in human retinitis pigmentosa. *Invest. Ophthalmol. Vis. Sci.* **51**, 5356–5364 (2010).
21. DeYoe, E.A. *et al.* Mapping striate and extrastriate visual areas in human cerebral cortex. *Proc. Natl. Acad. Sci. USA* **93**, 2382–2386 (1996).
22. Engel, S.A., Glover, G.H. & Wandell, B.A. Retinotopic organization in human visual cortex and the spatial precision of functional MRI. *Cereb. Cortex* **7**, 181–192 (1997).
23. Engel, S.A. *et al.* fMri of human visual cortex. *Nature* **369**, 525 (1994).
24. Sereno, M.I. *et al.* Borders of multiple visual areas in humans revealed by functional magnetic resonance imaging. *Science* **268**, 889–893 (1995).
25. Smirnakis, S.M. *et al.* Lack of long-term cortical reorganization after macaque retinal lesions. *Nature* **435**, 300–307 (2005).
26. Baker, C.I., Dilks, D.D., Peli, E. & Kanwisher, N. Reorganization of visual processing in macular degeneration: replication and clues about the role of foveal loss. *Vision Res.* **48**, 1910–1919 (2008).
27. Crossland, M.D., Morland, A.B., Feely, M.P., von dem Hagen, E. & Rubin, G.S. The effect of age and fixation instability on retinotopic mapping of primary visual cortex. *Invest. Ophthalmol. Vis. Sci.* **49**, 3734–3739 (2008).
28. Parrish, T.B., Gitelman, D.R., LaBar, K.S. & Mesulam, M.M. Impact of signal-to-noise on functional MRI. *Magn. Reson. Med.* **44**, 925–932 (2000).
29. Cavanaugh, J.R., Bair, W. & Movshon, J.A. Nature and interaction of signals from the receptive field center and surround in macaque V1 neurons. *J. Neurophysiol.* **88**, 2530–2546 (2002).
30. Dumoulin, S.O. & Wandell, B.A. Population receptive field estimates in human visual cortex. *Neuroimage* **39**, 647–660 (2008).
31. Andrews, T.J., Halpern, S.D. & Purves, D. Correlated size variations in human visual cortex, lateral geniculate nucleus, and optic tract. *J. Neurosci.* **17**, 2859–2868 (1997).
32. Hubel, D.H. & Wiesel, T.N. The period of susceptibility to the physiological effects of unilateral eye closure in kittens. *J. Physiol. (Lond.)* **206**, 419–436 (1970).
33. Hubel, D.H., Wiesel, T.N. & LeVay, S. Plasticity of ocular dominance columns in monkey striate cortex. *Phil. Trans. R. Soc. Lond. B* **278**, 377–409 (1977).
34. Le Vay, S., Wiesel, T.N. & Hubel, D.H. The development of ocular dominance columns in normal and visually deprived monkeys. *J. Comp. Neurol.* **191**, 1–51 (1980).
35. Horton, J.C. & Hocking, D.R. Timing of the critical period for plasticity of ocular dominance columns in macaque striate cortex. *J. Neurosci.* **17**, 3684–3709 (1997).
36. Williams, M.A. *et al.* Feedback of visual object information to foveal retinotopic cortex. *Nat. Neurosci.* **11**, 1439–1445 (2008).
37. Angelucci, A. & Bullier, J. Reaching beyond the classical receptive field of V1 neurons: horizontal or feedback axons? *J. Physiol. (Paris)* **97**, 141–154 (2003).
38. Angelucci, A. & Sainsbury, K. Contribution of feedforward thalamic afferents and corticogeniculate feedback to the spatial summation area of macaque V1 and LGN. *J. Comp. Neurol.* **498**, 330–351 (2006).
39. Lund, J.S. Anatomical organization of macaque monkey striate visual cortex. *Annu. Rev. Neurosci.* **11**, 253–288 (1988).
40. Gilbert, C.D. & Wiesel, T.N. Morphology and intracortical projections of functionally characterised neurones in the cat visual cortex. *Nature* **280**, 120–125 (1979).
41. Dougherty, R.F. *et al.* Visual field representations and locations of visual areas V1/2/3 in human visual cortex. *J. Vis.* **3**, 586–598 (2003).
42. Horton, J.C. & Hocking, D.R. Monocular core zones and binocular border strips in primate striate cortex revealed by the contrasting effects of enucleation, eyelid suture, and retinal laser lesions on cytochrome oxidase activity. *J. Neurosci.* **18**, 5433–5455 (1998).
43. Liu, T. *et al.* Incomplete cortical reorganization in macular degeneration. *Invest. Ophthalmol. Vis. Sci.* **51**, 6826–6834 (2010).
44. Boucard, C.C. *et al.* Changes in cortical grey matter density associated with long-standing retinal visual field defects. *Brain* **132**, 1898–1906 (2009).

ONLINE METHODS

Participants. Eight individuals with stabilized AMD (ages 70–90) and a further eight with the JMD (Stargardt's Disease) (ages 19–49) were recruited at the Moorfields Eye Hospital, London. All of the participants had established bilateral lesions for at least 1 year, with a central scotoma of less than 10-deg radius spanning the fovea and a stable preferred retinal locus. Visual field sensitivity and fixation ability for all participants were evaluated directly on the retina using an MP1 microperimeter (NIDEK). Location of the foveal center, preferred retinal locus coordinates and fixation stability (bivariate contour ellipse area of fixation measurements) were determined using methods outlined in Timberlake *et al.* (2005). The mean diameter of the absolute retinal lesion was also computed from the microperimetry maps.

Five age-matched participants (ages 61–77) were recruited as controls for the AMD group and seven age-matched participants (ages 18–37) as controls for the JMD group. A further 12 control participants (ages 18–41) were recruited for a follow up experiment simulating retinal lesions. All control participants had normal or corrected-to-normal vision. Experimental protocols were approved by the London Multicenter Research Ethics Committee, Royal Holloway University of London Ethics Committee and the York Neuroimaging Center Science and Ethics Committee.

Scanning. fMRI and structural MRI data were acquired using 8-channel, phase-array head coils on either a Siemens Trio 3 Tesla at the Combined Universities Brain Imaging Center (Royal Holloway University of London), or on a GE 3-Tesla Signa HD Excite scanner at the York Neuroimaging Center (University of York).

For structural data, multi-average, whole-head T1-weighted anatomical volumes were acquired for each participant (1.0–1.13 mm^3 isotropic). Sequences used were 3D-MDEFT on the Siemens Trio or 3D-FSPGR on the GE Signa; imaging parameters in both sequences provide good gray-white contrast allowing the segmentation of anatomical data into gray and white matter, and subsequent visualization in volume and inflated cortical views. For functional data, gradient recalled echo pulse sequences were used to measure T2* BOLD data (repetition time = 3,000 ms, echo time = 30 ms, field of view = 28.8 cm, 128 × 128 matrix, 25 contiguous slices with 3-mm slice thickness). Images were read out using an EPI sequence. Magnetization was allowed to reach a steady state by discarding the first five volumes, an automated feature on both the scanners used.

Stimuli. Computer-generated visual stimuli were presented using a LCD projector (Sanyo PLC-XP40L at Royal Holloway University of London, Dukane ImagePro 8942 at the University of York); stimuli were rear projected onto an acrylic screen situated in the bore of the MRI scanner, behind the participant's head. Participants viewed the stimuli via a mirror mounted on the head coil. Standard retinotopic mapping stimuli were used: a rotating wedge to map polar angle and an expanding annulus to map eccentricity[21–24]. Stimuli were generated with MATLAB (Mathworks) and controlled by MatVis (Neurometrics Institute). All stimuli were unmasked portions of a 100% contrast radial checkerboard with 8 rings and 24 radial segments on a mean gray background. Contrast reversal rate was 6 Hz. Each scan contained either the expanding annulus or rotating wedge. Projector throw was adjusted to stimulate the central 30 × 30 deg of visual angle (15-deg radius). The wedge stimulus was a 90-deg wedge of the flickering checkerboard, rotating about the center of the screen. The ring stimulus comprised three rings of the checkerboard that increased in angular extent (to a maximum of 15 deg). As it moved out from the center of the visual field; each ring was replaced by a new ring at the center as the existing ring approached the edge of the visual field. Both the wedge and ring stimuli had a period of 36 s and were repeated for seven full cycles.

Experiment 1. The standard expanding ring and rotating wedge stimuli described above were used. In addition, the position of a red fixation cross was manipulated to ensure that stimuli were centered on each individual participant's retina. For control participants, a red fixation cross was placed at the center of the stimulus. For the patient group, the cross was placed at each individual's stable preferred retinal locus, as measured by microperimetry. Four ring and four wedge datasets were typically collected for each participant during a single visit, except where participant discomfort or excessive movement required fewer scans. Only three scans were collected during the first session in two individuals with AMD and two individuals with JMD and only two scans were performed on one of the elderly controls. Scans were repeated in a second visit in most participants (20 out of 28). Four scans were again performed during the second session, except in two individuals with AMD (three scans) and four individuals with JMD (three had three scans, one had two scans).

Experiment 2. As in Experiment 1, standard retinotopic mapping stimuli were used. A red fixation cross was placed in the center of the stimulus. In separate scans, the 12 control participants were either shown the full stimulus (ring and wedge) or a masked version (of the rings) to simulate a central lesion. The mask consisted of a centrally placed static disk (7.5-deg radius) at mean luminance gray such that the central portion of the visual field was constant throughout the scan (**Fig. 3**). At least two scans were acquired for each condition. 10 of the 12 participants returned for a second scanning session on a separate date.

Data analysis. Data were analyzed using publicly available tools (http://white.stanford.edu/software/). Most data analysis was performed in Matlab using the mrVISTA toolbox. For anatomical data, the occipital cortices of acquired anatomical volumes were manually segmented into white and gray volumes (mrGray)[45]. The cortical surface (gray matter) of each subject was constructed and rendered in three dimensions from this segmentation using mrMesh/mrVista[46].

For function data, functional images were corrected for spatial inhomogeneity (mrInitRet). Motion correction was achieved using FSL's MCFLIRT[47]. Functional time series were high-pass filtered to remove baseline drifts. Percent signal change was computed for each voxel by dividing by and subtracting its mean amplitude value over time. The strength of stimulus-synchronized activity at each voxel was assessed using coherence. Coherence (C) is defined as the Fourier amplitude of the BOLD signal at the stimulus fundamental frequency ($f_0 = 7$) divided by the sum of amplitudes of frequency bins around the fundamental ($C = A(f_0) / \sum \sqrt{A(f)^2}$) (refs. 18–25). The visual field representation of each voxel in cortex was derived by using the Fourier phase at the stimulus frequency, corresponding to the relative delay of the cyclical response[22,48]. Functional data were averaged across scans for repeated scans (usually four) within a session for each individual. Functional data were manually aligned to the high-resolution anatomical volume and visualized in three dimensions.

ROIs were defined by an algorithm that gathered all contiguous gray matter in a circular patch 8 mm in diameter centered on a selected point in the high-resolution structural data. Three ROIs were chosen in each hemisphere of each participant based strictly on anatomical criteria: one at the occipital pole to represent activity from the fovea (the lesion projection zone in patients), one more anterior in the calcarine sulcus to represent activity from more peripheral retina (which is intact in patients) and one further anterior in the brain on the lateral aspect of the frontal lobes, serving as a control region in the first experiment. The mean coherence was calculated across voxels in an ROI for each individual and averaged across scans in each session. The fMRI noise distribution is not normal and may differ from one individual to the next or from one day to the next. To normalize the responses, the logarithm of the resulting coherence data was taken before averaging data across scanning sessions and across participants[49].

We assessed the degree to which the time series of any voxel in predefined regions of interest in the gray matter fitted a series of receptive field models as described previously[30]. Best fitting models were retained if they accounted for more than 15% of the variance of the time series of each voxel as in previous research[50]. The retained models were then averaged across voxels to give an overall measure of the population receptive field properties for each ROI. The data used for modeling were for the expanding ring stimuli only because it was for this presentation that we had a comparable number of runs across the participant groups, and it was the only stimulus that was masked to simulate retinal lesions. It is important to note that the candidate models were identical for all stimulus conditions and we did not restrict the receptive field models to any locations or sizes. The ROIs considered were calcarine sulcus, as specified above, and occipital pole, but in this case the diameter of occipital pole was 20 mm to gain increased sensitivity. Although the 20-mm diameter ROI might capture some signals from tissue receiving input from intact retina in patients with small retinal lesions, we ensured that for the control participants receiving full-field and simulated lesion stimulation, the occipital pole ROI only included voxels responding to eccentricities less than 7.5 deg when the full stimulus was presented.

doi:10.1038/nn.2793

We computed the area of primary visual cortex, A_M, that exhibited activity above a coherence threshold of 0.30 for all participants in the patient and control groups in whom we simulated retinal lesions. Using responses to rotating wedge stimuli, we first identified the cortical representations of the upper and lower vertical meridians marking the boundaries of V1 in each participant (see **Fig. 7**). We then defined a V1 ROI that was bounded by the extrapolation of the vertical meridians to the occipital pole and an anterior boundary that was just beyond the limit of activity in response to rotating wedges. This region was not restricted to those voxels that exceeded a specific threshold, but rather was a generously defined estimate of the extent of V1. Voxels in this V1 region that responded to rings at a coherence of greater than 0.30 were retained for the calculation of the area of significant activity in V1. The cortical area of activity was calculated using methods described previously[41]. We then computed a series of estimates of the predicted area of activation, A_P, based on the intact regions of visual field in patients (see **Fig. 7** for a schematic of the method). For each patient, we computed estimates from the corresponding group of age-matched controls (for example, for each individual with JMD we obtained seven estimates, one from each of the young control subjects). The mean predicted area, $\bar{A}_P$, was then computed. We repeated these computations to obtain $\bar{A}_P$ for controls with simulated central visual loss. Note that these computations were also based on the original data from the young control subjects. If remapping were to occur, A_M will exceed $\bar{A}_P$ and thus a ratio of the A_M to $\bar{A}_P$ will exceed unity. Using the ratio as our outcome measure is essential because it accounts for individual differences in retinal lesion size.

Statistical analyses. Statistics were calculated using functions in the MATLAB Statistical Toolbox. A two-way analysis of variance was performed on the averaged expanding ring data (for each session) for the elderly group and for the young group. Visual status (patient versus control) and ROI (occipital pole versus calcarine sulcus versus control region) were the independent variables and log coherence (fMRI response magnitude) was the dependent variable. A repeated-measures ANOVA was performed on the data to test for significant differences within subjects across two sessions. To test for age effects, a three-way analysis of variance was performed on the combined data, with age, visual status and ROI as factors. All ANOVAs employed a Type III sum of squares calculation, and all subsequent multiple comparisons were corrected using the Tukey-Kramer criterion, as appropriate for an unbalanced design with unequal number of subjects across groups. A multiple regression analysis was performed on the patient data to determine the effects of lesion size and age on log coherence responses for each ROI. For the receptive field analysis, we used Student *t* tests to evaluate group differences in eccentricity and size of the receptive fields and sampling probability at each cortical location. Linear regression was used to assess the relationship between eccentricity and size of population receptive fields in the occipital pole ROI; 95% confidence intervals in the linear correlation parameters was estimated using jackknife resampling, taking into consideration the unequal number of points contributed by each participant. For the cortical area measures in **Figure 7**, group effects and deviations of the area ratio from unity were evaluated using *t* tests and ANOVAs, respectively.

45. Teo, P.C., Sapiro, G. & Wandell, B.A. Creating connected representations of cortical gray matter for functional MRI visualization. *IEEE Trans. Med. Imaging* **16**, 852–863 (1997).
46. Wandell, B.A., Chial, S. & Backus, B.T. Visualization and measurement of the cortical surface. *J. Cogn. Neurosci.* **12**, 739–752 (2000).
47. Jenkinson, M., Bannister, P., Brady, M. & Smith, S. Improved optimization for the robust and accurate linear registration and motion correction of brain images. *Neuroimage* **17**, 825–841 (2002).
48. Wandell, B.A., Brewer, A.A. & Dougherty, R.F. Visual field map clusters in human cortex. *Phil. Trans. R. Soc. Lond. B* **360**, 693–707 (2005).
49. Lewis, S.M. *et al.* Logarithmic transformation for high-field BOLD fMRI data. *Exp. Brain Res.* **165**, 447–453 (2005).
50. Winawer, J., Horiguchi, H., Sayres, R.A., Amano, K. & Wandell, B.A. Mapping hV4 and ventral occipital cortex: the venous eclipse. *J. Vis.* **10**, 1–22 (2010).